NACA

RESEARCH MEMORANDUM

A THEORETICAL INVESTIGATION OF THE DYNAMIC LATERAL OSCILLATORY STABILITY OF AN AIRPLANE HAVING A 60° TRIANGULAR WING

By Joseph L. Johnson

Langley Aeronautical Laboratory
Langley Air Force Base, Va.

NATIONAL ADVISORY COMMITTEE FOR AERONAUTICS

WASHINGTON
March 8, 1950

NATIONAL ADVISORY COMMITTEE FOR AERONAUTICS

RESEARCH MEMORANDUM

A THEORETICAL INVESTIGATION OF THE DYNAMIC LATERAL OSCILLATORY STABILITY OF AN AIRPLANE HAVING A 60° TRIANGULAR WING

By Joseph L. Johnson

SUMMARY

A theoretical study has been made of the dynamic lateral stability characteristics of an airplane having a 60° triangular wing. The calculations included the determination of the neutral-lateral-oscillatory-stability boundary (R = 0), the period and time to damp to one-half amplitude of the lateral oscillation, and the time to damp to one-half amplitude for the spiral mode. Factors varied in the investigation were lift coefficient and altitude. Since small changes in some of the mass and aerodynamic characteristics may cause considerable differences in the lateral stability of an airplane, it is well to keep in mind that the results presented herein apply only to an airplane having the characteristics for which the calculations were made.

The results of the investigation showed that the lateral oscillation of the airplane was stable over the lift-coefficient range at sea level and at an altitude of 30,000 feet. The damping of the lateral oscillation met the U. S. Air Force requirements for all conditions except in the low-lift-coefficient range at 30,000 feet. The airplane was spirally stable for all conditions.

INTRODUCTION

A theoretical study has been made of the dynamic lateral stability characteristics of an airplane having a 60° triangular wing. A three-view sketch of the airplane is shown in figure 1. The analysis was made by the Langley free-flight-tunnel staff and the calculations were made at the Langley Laboratory on a relay computer.

Calculations were made to determine the neutral-lateral-oscillatory-stability boundary ($R = 0$), the period and time to damp to one-half amplitude of the lateral oscillation, and the time to damp to one-half amplitude for the spiral mode for the airplane over the lift-coefficient range with a gross weight of 14,114 pounds at sea level and at an altitude of 30,000 feet. The results of the investigation are presented in the form of stability charts where the boundaries $R = 0$ are plotted as functions of the effective dihedral parameter $-C_{l_\beta}$ and the directional-stability parameter C_{n_β}. The period and time to damp to one-half amplitude are presented as functions of lift coefficient.

Recent theoretical investigations (reference 1) have shown that small changes in some of the mass and aerodynamic characteristics may cause considerable differences in the lateral stability of an airplane and it is well to keep in mind that the results presented herein apply only to an airplane having the characteristics for which the calculations were made.

SYMBOLS AND COEFFICIENTS

S	wing area, square feet
$\bar{c}$	mean aerodynamic chord, feet
V	airspeed, feet per second
b	wing span, feet
q	dynamic pressure, pounds per square foot
ρ	air density, slugs per cubic foot
W	weight, pounds
g	acceleration of gravity, feet per second per second
m	mass, slugs (W/g)
μ_b	relative density factor based on wing span $(m/\rho Sb)$
α	angle of attack of reference axis (fig. 2), degrees
η	angle of attack of principal longitudinal axis of airplane, positive when principal axis is above flight path at the nose (fig. 2), degrees

ϵ angle between reference axis and principal axis, positive when reference axis is above principal axis at the nose (fig. 2), degrees

θ angle between reference axis and horizontal axis, positive when reference axis is above horizontal axis at the nose (fig. 2), degrees

γ angle of flight to horizontal axis, positive in a climb (fig. 2), degrees

Ψ angle of yaw, degrees or radians

β angle of sideslip, degrees or radians

ϕ angle of bank, radians

R Routh's discriminant ($R = BCD - AD^2 - B^2E$ where A, B, C, D, and E are constants representing coefficients of the lateral-stability equation)

k_{X_o} radius of gyration about principal longitudinal axis, feet

k_{Z_o} radius of gyration about principal vertical axis, feet

K_{X_o} nondimensional radius of gyration about principal longitudinal axis $\left(k_{X_o}/b\right)$

K_{Z_o} nondimensional radius of gyration about principal vertical axis $\left(k_{Z_o}/b\right)$

K_X nondimensional radius of gyration about longitudinal stability axis $\left(\sqrt{K_{X_o}{}^2\cos^2\eta + K_{Z_o}{}^2\sin^2\eta}\right)$

K_Z nondimensional radius of gyration about vertical stability axis $\left(\sqrt{K_{Z_o}{}^2\cos^2\eta + K_{X_o}{}^2\sin^2\eta}\right)$

K_{XZ} nondimensional product-of-inertia parameter $\left(\left(K_{Z_o}{}^2 - K_{X_o}{}^2\right)\cos\eta \sin\eta\right)$

[redacted]

C_L lift coefficient (Lift/qS)

C_n yawing-moment coefficient (Yawing moment/qSb)

C_l rolling-moment coefficient (Rolling moment/qSb)

C_Y lateral-force coefficient (Lateral force/qS)

C_{Y_β} rate of change of lateral-force coefficient with angle of sideslip, per degree or per radian, as specified $(\partial C_Y/\partial\beta)$

C_{n_β} rate of change of yawing-moment coefficient with angle of sideslip, per degree or per radian, as specified $(\partial C_n/\partial\beta)$

C_{l_β} rate of change of rolling-moment coefficient with angle of sideslip, per degree or per radian, as specified $(\partial C_l/\partial\beta)$

C_{Y_p} rate of change of lateral-force coefficient with rolling-angular-velocity factor, per radian $\left(\frac{\partial C_Y}{\partial \frac{pb}{2V}}\right)$

C_{l_p} rate of change of rolling-moment coefficient with rolling-angular-velocity factor, per radian $\left(\frac{\partial C_l}{\partial \frac{pb}{2V}}\right)$

C_{n_p} rate of change of yawing-moment coefficient with rolling-angular-velocity factor, per radian $\left(\frac{\partial C_n}{\partial \frac{pb}{2V}}\right)$

C_{l_r} rate of change of rolling-moment coefficient with yawing-angular-velocity factor, per radian $\left(\frac{\partial C_l}{\partial \frac{rb}{2V}}\right)$

C_{n_r} rate of change of yawing-moment coefficient with yawing-angular-velocity factor, per radian $\left(\frac{\partial C_n}{\partial \frac{rb}{2V}}\right)$

[redacted]

C_{Y_r} rate of change of lateral-force coefficient with yawing-angular-velocity factor, per radian $\left(\frac{\partial C_Y}{\partial \frac{rb}{2V}}\right)$

l tail length (distance from center of gravity to rudder hinge line), feet

$\overline{z}$ height of center of pressure of vertical tail above fuselage axis, feet

p rolling angular velocity, radians per second

r yawing angular velocity, radians per second

D_b differential operator (d/ds_b)

s_b distance along flight path, spans (Vt/b)

λ complex root of stability equation $(c \pm id)$

t time, seconds

P period of oscillation, seconds

$T_{1/2}$ time for amplitude of oscillation to change by factor of 2 (positive value indicates a decrease to half amplitude, negative value indicates an increase to double amplitude)

$C_{1/2}$ cycles for amplitude of oscillation to change by factor of 2 (positive value indicates a decrease to half amplitude, negative value indicates an increase to double amplitude)

EQUATIONS OF MOTION

The nondimensional lateral equations of motion (reference 1), referred to a stability-axes system (fig. 3), are:

In roll

$$2\mu_b\left(K_X^2 D_b^2\phi + K_{XZ} D_b^2 \psi\right) = C_{l_\beta}\beta + \frac{1}{2}C_{l_p} D_b\phi + \frac{1}{2}C_{l_r} D_b\psi$$

[redacted]

In yaw

$$2\mu_b\left(K_Z^2 D_b^2\psi + K_{XZ} D_b^2\phi\right) = C_{n_\beta}\beta + \frac{1}{2}C_{n_p} D_b\phi + \frac{1}{2}C_{n_r} D_b\psi$$

In sideslip

$$2\mu_b(D_b\beta + D_b\psi) = C_{Y_\beta}\beta + \frac{1}{2}C_{Y_p} D_b\phi + C_L\phi + \frac{1}{2}C_{Y_r} D_b\psi + (C_L \tan\gamma)\psi$$

When $\phi_o e^{\lambda s_b}$ is substituted for ϕ, $\psi_o e^{\lambda s_b}$ for ψ, and $\beta_o e^{\lambda s_b}$ for β in the equations written in determinant form, λ must be a root of the stability equation

$$A\lambda^4 + B\lambda^3 + C\lambda^2 + D\lambda + E = 0 \qquad (1)$$

where

$$A = 8\mu_b^3\left(K_X^2 K_Z^2 - K_{XZ}^2\right)$$

$$B = -2\mu_b^2\left(2K_X^2 K_Z^2 C_{Y_\beta} + K_X^2 C_{n_r} + K_Z^2 C_{l_p} - 2K_{XZ}^2 C_{Y_\beta} - K_{XZ} C_{l_r} - K_{XZ} C_{n_p}\right)$$

$$C = \mu_b\Big(K_X^2 C_{n_r} C_{Y_\beta} + 4\mu_b K_X^2 C_{n_\beta} + K_Z^2 C_{l_p} C_{Y_\beta} + \frac{1}{2}C_{n_r} C_{l_p} - K_{XZ} C_{l_r} C_{Y_\beta} - 4\mu_b K_{XZ} C_{l_\beta}$$

$$- C_{n_p} K_{XZ} C_{Y_\beta} - \frac{1}{2}C_{n_p} C_{l_r} + K_{XZ} C_{n_\beta} C_{Y_p} - K_Z^2 C_{Y_p} C_{l_\beta} - K_X^2 C_{Y_r} C_{n_\beta} + K_{XZ} C_{Y_r} C_{l_\beta}\Big)$$

$$D = -\frac{1}{4}C_{n_r} C_{l_p} C_{Y_\beta} - \mu_b C_{l_p} C_{n_\beta} + \frac{1}{4}C_{n_p} C_{l_r} C_{Y_\beta} + \mu_b C_{n_p} C_{l_\beta} + 2\mu_b C_L K_{XZ} C_{n_\beta}$$

$$- 2\mu_b C_L K_Z^2 C_{l_\beta} - 2\mu_b K_X^2 C_{n_\beta} C_L \tan\gamma + 2\mu_b K_{XZ} C_{l_\beta} C_L \tan\gamma + \frac{1}{4}C_{l_p} C_{n_\beta} C_{Y_r}$$

$$- \frac{1}{4}C_{n_p} C_{l_\beta} C_{Y_r} - \frac{1}{4}C_{l_r} C_{n_\beta} C_{Y_p} + \frac{1}{4}C_{n_r} C_{l_\beta} C_{Y_p}$$

$$E = \frac{1}{2}C_L\left(C_{n_r} C_{l_\beta} - C_{l_r} C_{n_\beta}\right) + \frac{1}{2}C_L \tan\gamma\left(C_{l_p} C_{n_\beta} - C_{n_p} C_{l_\beta}\right)$$

The damping and period of the lateral oscillation in seconds are given, respectively, by the equations $T_{1/2} = -\frac{0.69}{c}\frac{b}{V}$ and $P = \frac{2\pi}{d}\frac{b}{V}$ where c and d are the real and imaginary parts of the complex root of the stability equation. The damping of the spiral mode is determined similarly from one of the two real roots (usually the less stable one) of the stability equation.

The conditions for neutral-oscillatory stability as shown in reference 2 are that the coefficients of the stability equation satisfy Routh's discriminant set equal to zero

$$R = BCD - AD^2 - B^2E = 0$$

and that the coefficients B and D have the same sign. In general, the sign of the coefficient B is determined by the factors $-C_{Y_\beta}$, $-C_{n_r}$, and $-C_{l_p}$ which appear in the predominant terms of B. Thus, B is positive in the usual case in which there is positive weathercock stability and positive damping in roll. Hence, the coefficient D must be positive if R = 0 is a neutral-oscillatory-stability boundary.

Calculations

Calculations were made to determine the neutral-lateral-oscillatory-stability boundary (R = 0), the period and time to damp to one-half amplitude for the lateral oscillation, and the time to damp to one-half amplitude for the spiral mode over a lift-coefficient range (0.1, 0.5, and 1.00) for the airplane with a gross weight of 14,114 pounds at sea level and at an altitude of 30,000 feet.

The aerodynamic and mass characteristics used in the calculations are presented in table I. Values of $C_{n_\beta(\text{tail off})}$ and $C_{Y_\beta(\text{tail off})}$ were taken from force tests made on a similar configuration in the Ames 40-by 80-foot tunnel. The tail-off values of C_{n_r}, C_{l_r}, C_{n_p}, and C_{l_p} were estimated from reference 3 and from unpublished experimental data obtained in the Langley stability tunnel. The contributions of the tail to the stability derivatives were estimated from the equations given in the footnote of table I and are similar to those given in reference 4. The estimated values of C_{n_p} for the complete model for a lift coefficient of 0.1 and 0.5 are in reasonable agreement with

experimental data from the Langley stability tunnel, but no reliable experimental data are available for comparison with the calculated value for a lift coefficient of 1.0.

The roots of the stability equation were computed to determine the period and time to damp to one-half amplitude for each condition for which a boundary was calculated. Presented in table II are the aerodynamic and mass characteristics used in computing the roots of the stability equations. The values are essentially the same as those given in table I except that the mass characteristics are presented in a different form and the total derivatives are given for each condition.

RESULTS AND DISCUSSION

The results of the calculations are presented in figures 4 to 10. All results are presented in terms of lift coefficient and figure 9 is presented for convenience in interpreting the results in terms of airspeed. Figure 10 is presented to show how the damping of the airplane compares with the damping requirements of the U. S. Air Force.

Neutral-Lateral-Oscillatory-Stability Boundaries

The effect of lift coefficient on the neutral-lateral-oscillatory-stability boundaries (R = 0) is presented in figures 4 and 5 for the airplane at sea level and 30,000 feet, respectively. The symbols on these figures represent the C_{n_β} and $-C_{l_\beta}$ values for the airplane at each lift coefficient. Figure 4 shows that the airplane was oscillatorily stable for each lift coefficient and that the boundary shifted downward with an increase in lift coefficient.

Increasing the altitude to 30,000 feet produced very little change in the position of the R = 0 boundary for a given lift coefficient as shown by a comparison of figures 4 and 5. A small destabilizing shift of the boundary occurred at $C_L = 0.10$ and was the largest change in the boundary over the lift-coefficient range.

Period and Damping of the Lateral Oscillation

The effect of lift coefficient on the reciprocal of the time to damp to one-half amplitude and the period of the lateral oscillation is presented in figures 6 and 7, respectively, and the results are tabulated in table III. The airplane is stable for all conditions of altitude and lift coefficient with the greatest damping occurring at sea level. The

results of figure 7 show very little change in the period of the oscillations with change in altitude.

Presented in figure 8 are the damping characteristics of the airplane in terms of cycles. The cycles to damp are determined by dividing the time to damp by the period. If the value of $\frac{1}{C_{1/2}}$ is greater than 0.50 it means that the lateral oscillation damps in 2 cycles or less. It is seen from this figure that the lateral oscillation damps in 2 cycles or less for all conditions except at a lift coefficient of 0.10 at an altitude of 30,000 feet.

Presented in figure 10 are the calculated damping characteristics for the airplane in comparison with the required damping specifications of the U. S. Air Force (reference 5). The symbols in this figure represent the points under consideration for the airplane and show that the conditions investigated meet the Air Force requirements for satisfactory damping except at the low lift coefficients at an altitude of 30,000 feet.

Spiral Stability

The reciprocal of the time to damp to one-half amplitude for the spiral (aperiodic) mode is presented in table III. It is seen that the spiral mode is slightly stable over the low and medium lift-coefficient range. At a lift coefficient of 1.00 the aperiodic mode disappears and a stable long-period oscillation occurs. The sea-level condition showed the greatest amount of spiral stability over the lift-coefficient range and increasing the lift coefficient increased the spiral stability for both the sea-level and 30,000-foot-altitude conditions.

The Air Force flying-qualities requirements do not call for spiral stability, but state that the spiral mode should not double amplitude in less than 4 seconds. It is therefore concluded that an airplane of this type will have satisfactory spiral stability for the conditions investigated.

CONCLUDING REMARKS

The results of the investigation are summarized in the following paragraphs. Since small changes in some of the mass and aerodynamic characteristics may cause considerable differences in the lateral stability of an airplane, the results apply only to a 60° triangular-wing airplane in the condition for which the calculations were made.

[redacted]

1. The lateral oscillatory stability was satisfactory over the lift-coefficient range for the airplane at sea level.

2. Increasing altitude decreased the damping for all lift coefficients. The airplane was stable at an altitude of 30,000 feet, but did not meet the U. S. Air Force specifications over the low-lift-coefficient range.

3. The airplane was spirally stable for all conditions.

Langley Aeronautical Laboratory
National Advisory Committee for Aeronautics
Langley Air Force Base, Va.

REFERENCES

1. Sternfield, Leonard: Some Considerations of the Lateral Stability of High-Speed Aircraft. NACA TN 1282, 1947.

2. Routh, Edward John: Dynamics of a System of Rigid Bodies. Part II. Sixth ed., rev. and enl., Macmillan and Co., Ltd., 1905. (Reprinted 1930.)

3. Toll, Thomas A., and Queijo, M. J.: Approximate Relations and Charts for Low-Speed Stability Derivatives of Swept Wings. NACA TN 1581, 1948.

4. Bamber, Millard J.: Effect of Some Present-Day Airplane Design Trends on Requirements for Lateral Stability. NACA TN 814, 1941.

5. Anon.: Flying Qualities of Piloted Airplanes. U. S. Air Force Specification No. 1815-B, June 1, 1948.

[redacted]

[redacted]

TABLE I

CHARACTERISTICS OF A 60° TRIANGULAR-WING AIRPLANE USED IN DETERMINING THE NEUTRAL-LATERAL-OSCILLATORY-STABILITY BOUNDARIES

[b = 31.30 ft; S = 425.00 sq ft; W = 14114.0 lb; γ = 0°; $\frac{l}{b}$ = 0.240; C_{Y_p} = 0; C_{Y_r} = 0; $C_{Y_{\beta_{tail}}}$ = −0.8 to 0.8; $\frac{\bar{x}}{b}$ = 0.207 to 0.088]

Altitude	C_L	α	ϵ	η	μ_b	k_{X_o}	k_{Z_o}	ρ	$C_{Y_{\beta(\text{tail off})}}$	$C_{n_{\beta(\text{tail off})}}$	$C_{l_{p(\text{tail off})}}$	$C_{n_{p(\text{tail off})}}$	$C_{l_{r(\text{tail off})}}$	$C_{n_{r(\text{tail off})}}$
Sea level	0.1	2.2	5.1	−2.9	13.83	3.86	9.48	0.00238	−0.1146	−0.055	−0.15	0.005	0.010	−0.010
	.5	11.6	5.1	6.5	13.83	3.86	9.48	0.00238	−.200	−.040	−.10	.030	.018	−.022
	1.00	23.2	5.1	18.1	13.83	3.86	9.48	0.00238	−.573	−.100	−.10	.040	−.172	−.166
30,000 ft	.1	2.2	5.1	−2.9	37.03	3.86	9.48	0.000889	−0.1146	−0.055	−0.15	0.005	0.010	−0.010
	.5	11.6	5.1	6.5	37.03	3.86	9.48	.000889	−.200	−.040	−.10	.030	.018	−.022
	1.00	23.2	5.1	18.1	37.03	3.86	9.48	.000889	−.573	−.100	−.10	.040	−.172	−.166

Tail contributions are determined from the following equations:

$$C_{l_{p(C_{n_\beta}=0)}} = C_{l_{p(\text{tail off})}} - 2\left(\frac{\bar{x}}{b} - \frac{l}{b}\sin\alpha\right)^2 \frac{b}{l}\left(-C_{n_{\beta_{\text{tail off}}}}\right)$$

$$C_{l_{p_{total}}} = C_{l_{p(C_{n_\beta}=0)}} - 2\left(\frac{\bar{x}}{b} - \frac{l}{b}\sin\alpha\right)^2 \frac{b}{l} C_{n_\beta}$$

$$C_{l_{r(C_{n_\beta}=0)}} = C_{l_{r(\text{tail off})}} + 2\left(\frac{\bar{x}}{b} - \frac{l}{b}\sin\alpha\right)\left(-C_{n_{\beta_{\text{tail off}}}}\right)$$

$$C_{l_{r_{total}}} = C_{l_{r(C_{n_\beta}=0)}} + 2\left(\frac{\bar{x}}{b} - \frac{l}{b}\sin\alpha\right) C_{n_\beta}$$

$$C_{n_{p(C_{n_\beta}=0)}} = C_{n_{p(\text{tail off})}} + 2\left(\frac{\bar{x}}{b} - \frac{l}{b}\sin\alpha\right)\left(-C_{n_{\beta_{\text{tail off}}}}\right)$$

$$C_{n_{p_{total}}} = C_{n_{p(C_{n_\beta}=0)}} + 2\left(\frac{\bar{x}}{b} - \frac{l}{b}\sin\alpha\right) C_{n_\beta}$$

$$C_{n_{r(C_{n_\beta}=0)}} = C_{n_{r(\text{tail off})}} - 2\frac{l}{b}\left(-C_{n_{\beta_{\text{tail off}}}}\right)$$

$$C_{n_{r_{total}}} = C_{n_{r(C_{n_\beta}=0)}} - 2\frac{l}{b} C_{n_\beta}$$

[redacted]

NACA

[redacted]

TABLE II

CHARACTERISTICS OF A 60° TRIANGULAR-WING AIRPLANE USED IN DETERMINING THE PERIOD AND TIME TO DAMP TO ONE-HALF AMPLITUDE

$\left[C_{Y_p} = 0;\ C_{Y_r} = 0;\ \gamma = 0^\circ\right]$

Altitude	C_L	η	μ_b	$\left(\frac{k_{Y_o}}{b}\right)^2$	$\left(\frac{k_{Z_o}}{b}\right)^2$	K_X^2	K_Z^2	K_{XZ}	$C_{l_{p_{total}}}$	$C_{Y_{\beta_{total}}}$	$C_{l_{r_{total}}}$	$C_{n_{p_{total}}}$	$C_{n_{r_{total}}}$	$m/\rho SV$
Sea level	0.10	-2.9	13.83	0.0152	0.0916	0.0154	0.0914	-0.00386	-0.1772	-0.688	0.0466	0.0416	-0.0590	0.821
	.50	6.5	--do-	--do--	--do--	.0161	.0904	.0086	-.1125	-.715	.0396	.0515	-.0591	1.840
	1.00	18.1	--do-	--do--	--do--	.0225	.0842	.0226	-.1109	-.860	-.1437	.0683	-.2390	2.590
30,000 ft	0.10	-2.9	37.03	0.0152	0.0916	0.0154	0.0914	-0.00386	-0.1772	-0.688	0.0466	0.0416	-0.0590	1.342
	.50	6.5	--do-	--do--	--do--	.0161	.0904	.0086	-.1125	-.715	.0396	.0515	-.0591	3.001
	1.00	18.1	--do-	--do--	--do--	.0225	.0842	.0226	-.1109	-.860	-.1437	.0683	-.2390	4.245

[redacted]

TABLE III

PERIOD AND RECIPROCAL OF TIME TO DAMP TO ONE-HALF AMPLITUDE FOR A 60° TRIANGULAR-WING AIRPLANE

Altitude	C_L	C_{n_β} (per deg)	$-C_{l_\beta}$ (per deg)	Oscillatory mode			Aperiodic (spiral) mode
				Period	$\frac{1}{T_{1/2}}$ (1/sec)	$\frac{1}{C_{1/2}}$ (1/cycles)	$\frac{1}{T_{1/2}}$ (1/sec)
Sea level	0.10	0.00083	0.00085	2.97	0.314	0.935	0.00790
	.50	.000647	.00165	4.66	.361	1.67	.109
	1.00	.000912	.000953	4.87	.389	1.89	-------
				20.66	.389	8.06	-------
30,000 ft	.10	.00083	.00085	3.02	.141	.426	.00490
	.50	.000647	.00165	4.45	.240	1.06	.0557
	1.00	.000912	.000953	4.76	.234	1.11	-------
				34.86	.240	8.33	-------

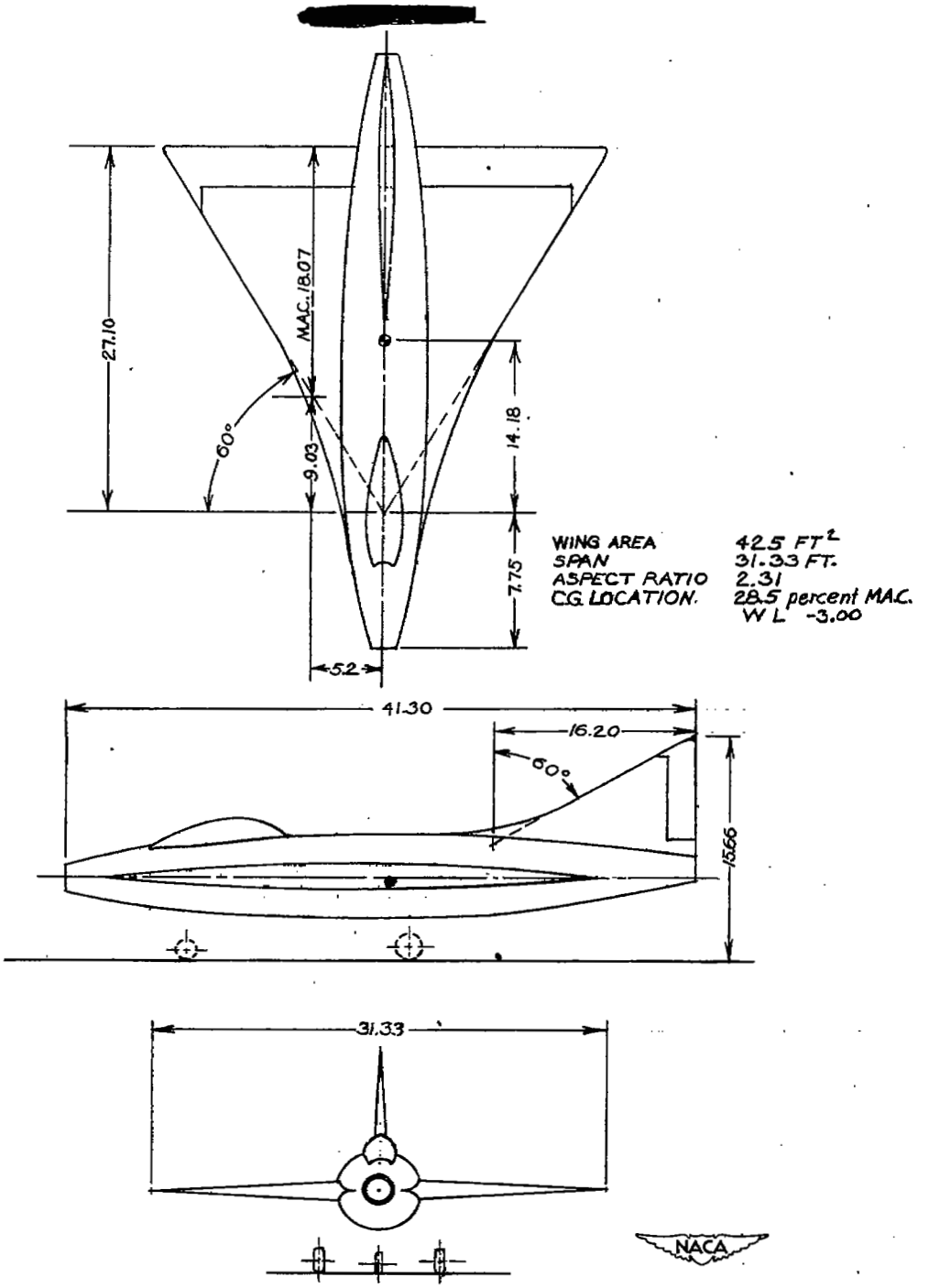

Figure 1.— Three-view drawing of the 60° triangular-wing airplane used in the investigation. All dimensions are in feet.

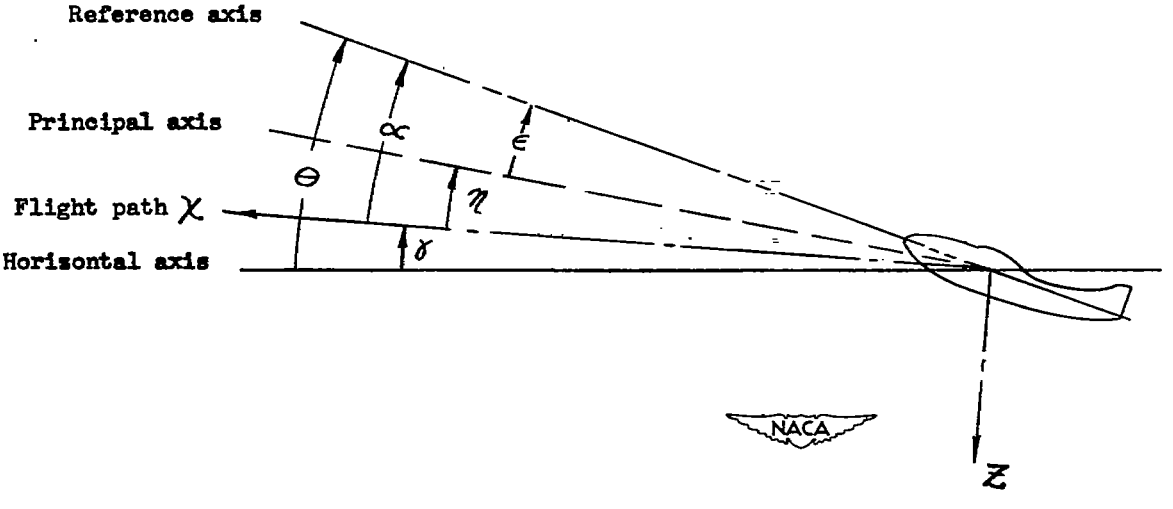

Figure 2.— System of axes and angular relationship in flight. Arrows indicate positive direction of angles. $\eta = \theta - \gamma - \epsilon$.

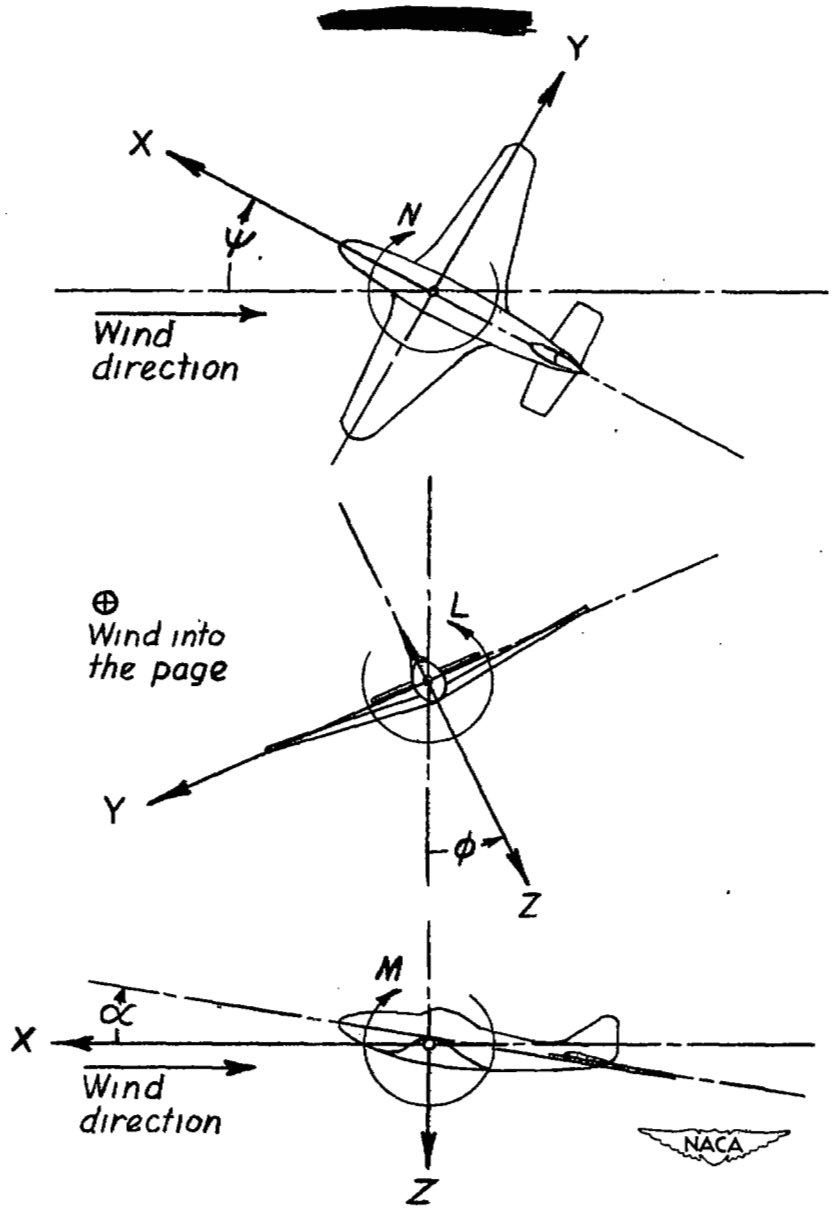

Figure 3.— The stability system of axes is defined as an orthogonal system of axes having their origin at the center of gravity and in which the Z-axis is in the plane of symmetry and perpendicular to the relative wind, the X-axis is in the plane of symmetry and perpendicular to the Z-axis, and the Y-axis is perpendicular to the plane of symmetry. Arrows indicate positive directions of moments and forces.

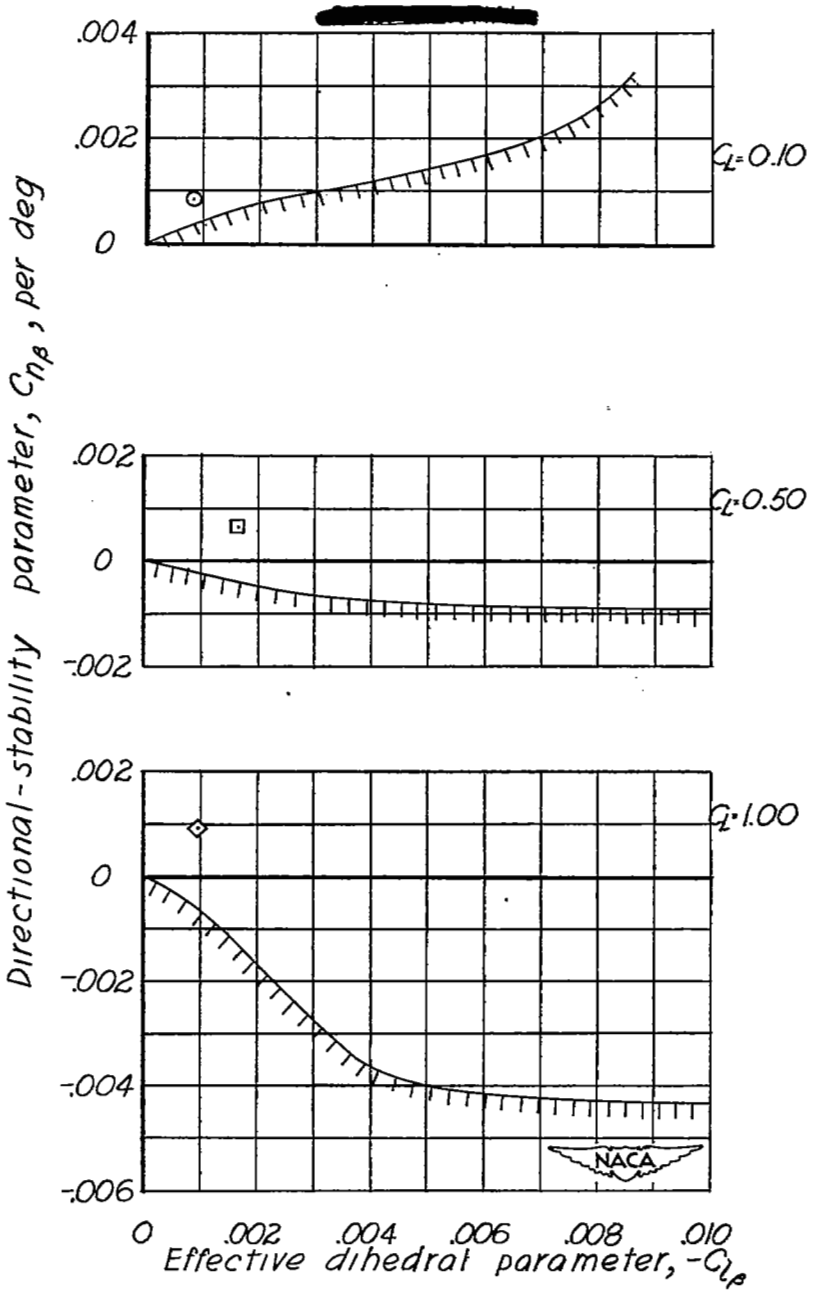

Figure 4.– Effect of lift coefficient on the neutral–lateral–oscillatory–stability boundary (R = 0) for the 60° triangular–wing airplane. Sea–level condition.

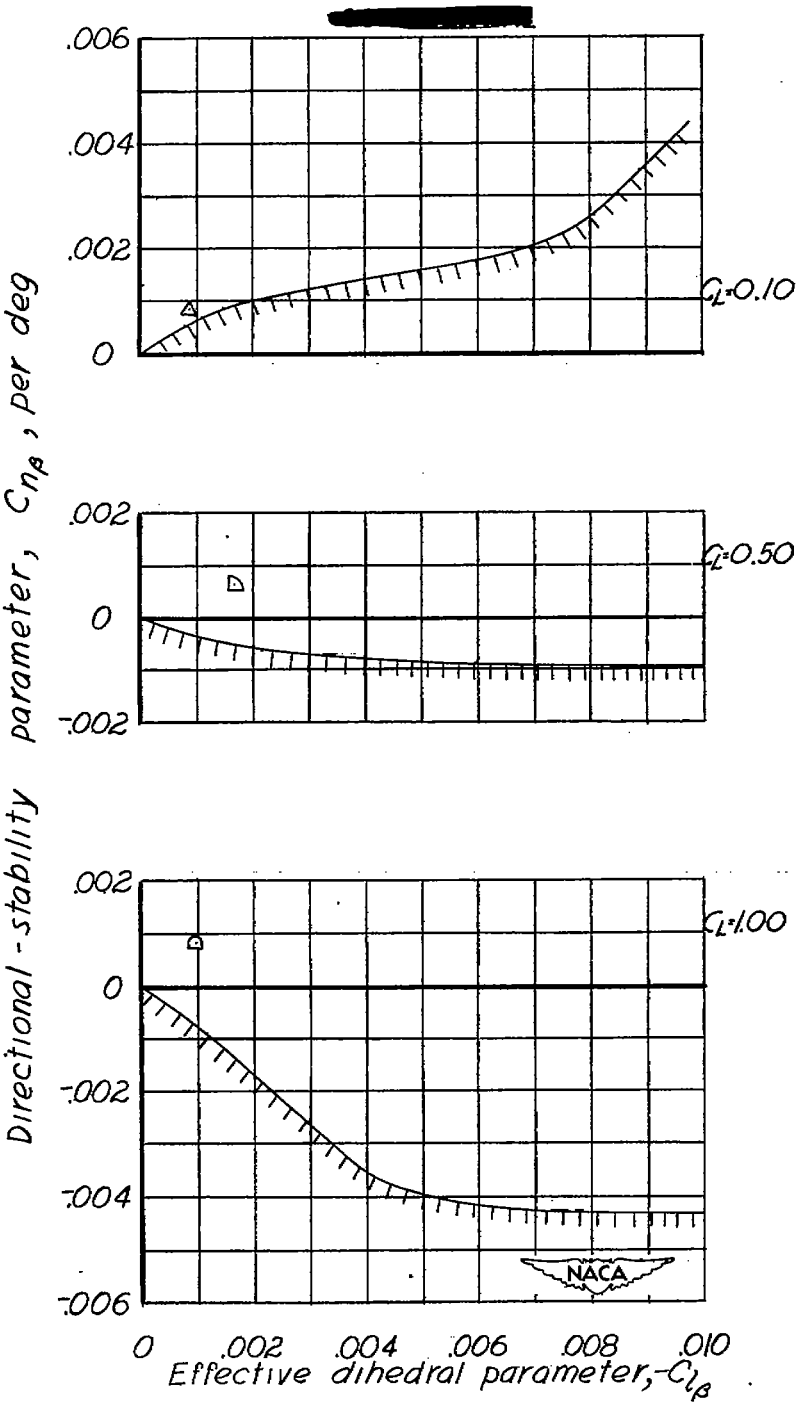

Figure 5.— Effect of lift coefficient on the neutral—lateral—oscillatory—stability boundary (R = 0) for the 60° triangular—wing airplane. 30,000—foot altitude.

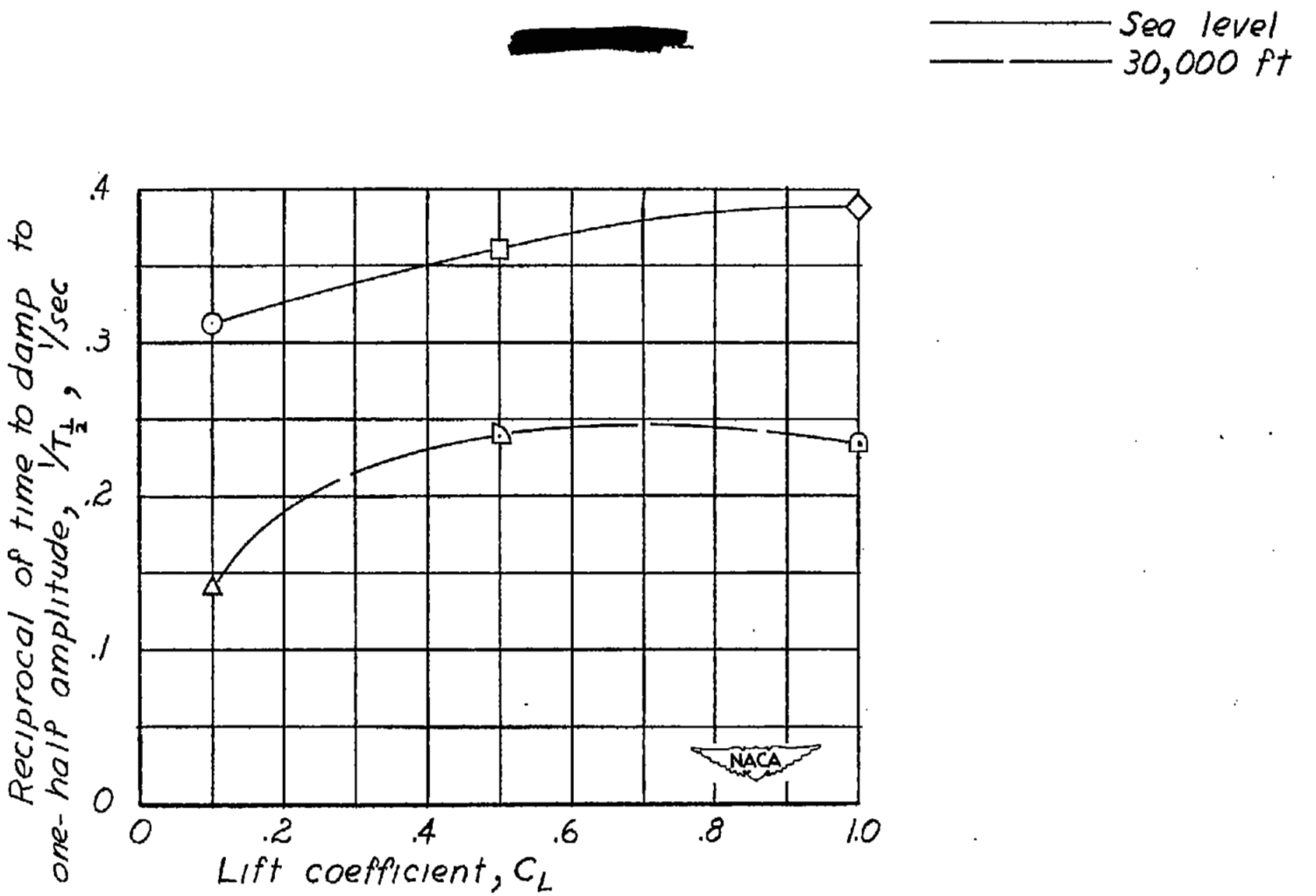

Figure 6.– Effect of lift coefficient on the reciprocal of the time to damp to one-half amplitude of the lateral oscillation for the 60° triangular-wing airplane.

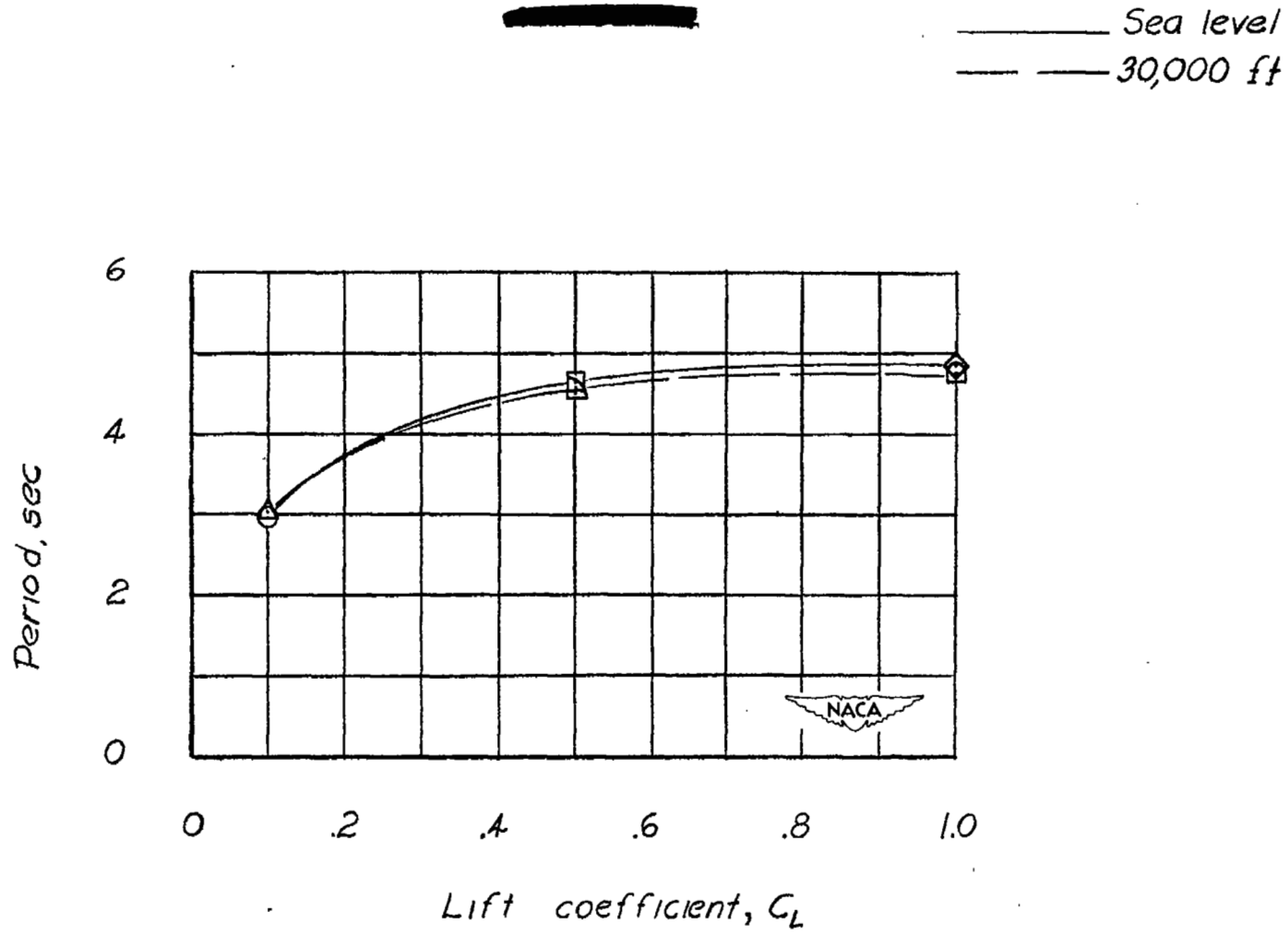

Figure 7.- Effect of lift coefficient on the period of the lateral oscillation for the 60° triangular-wing airplane.

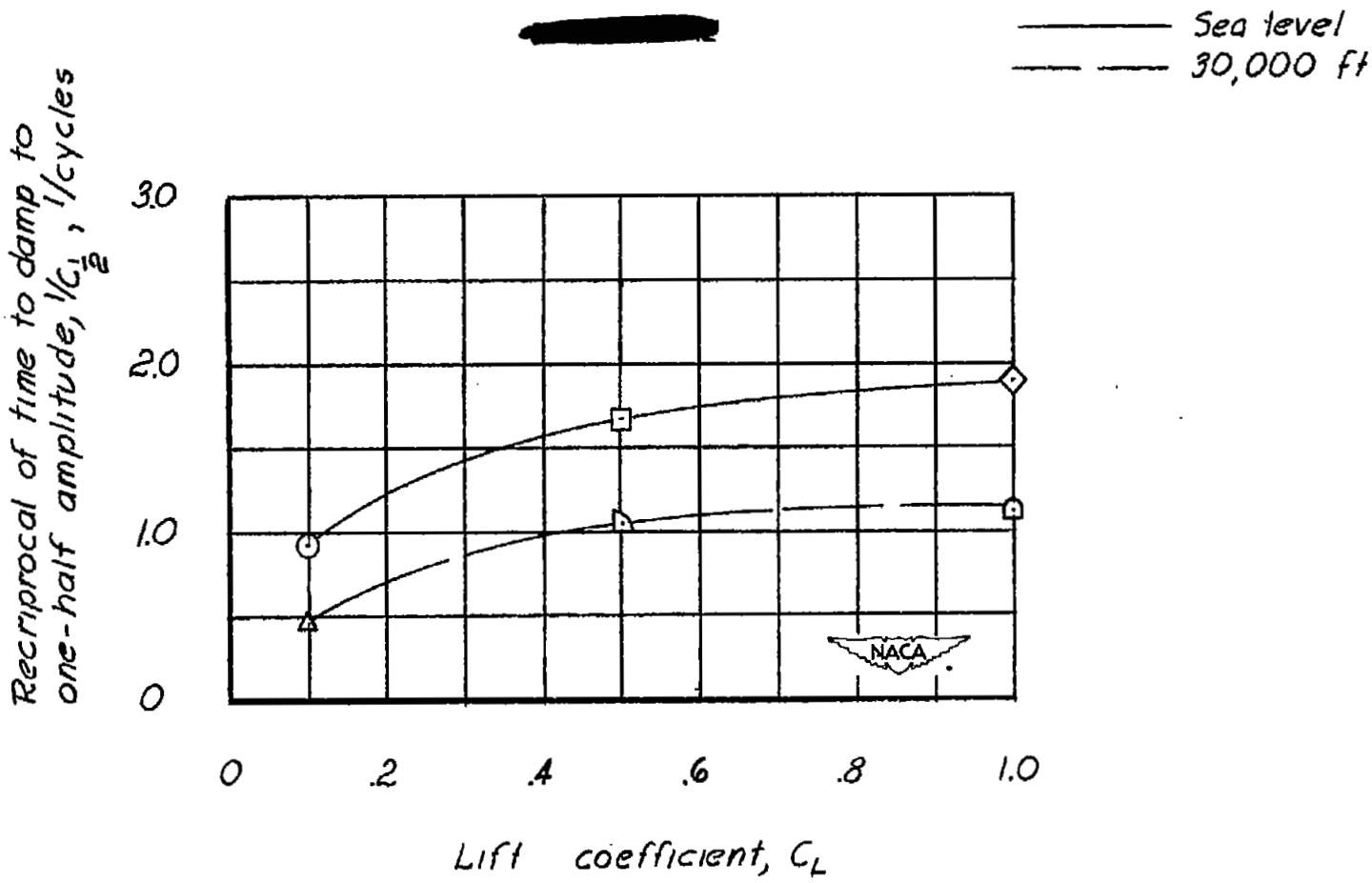

Figure 8.– Effect of lift coefficient on the reciprocal of the cycles to damp to one-half amplitude of the lateral oscillation for the 60° triangular-wing airplane.

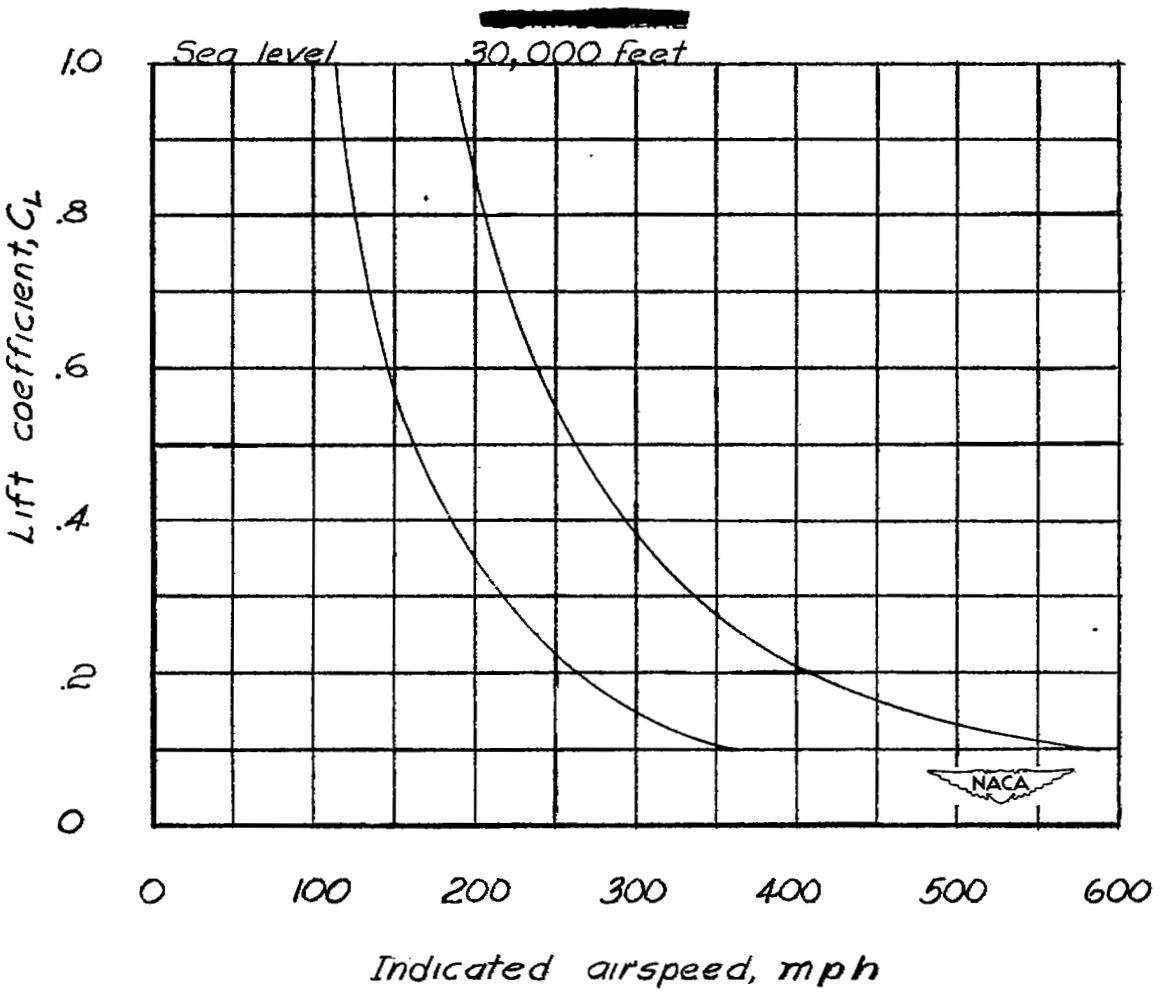

Figure 9.— Variation of lift coefficient with airspeed for the 60° triangular-wing airplane.

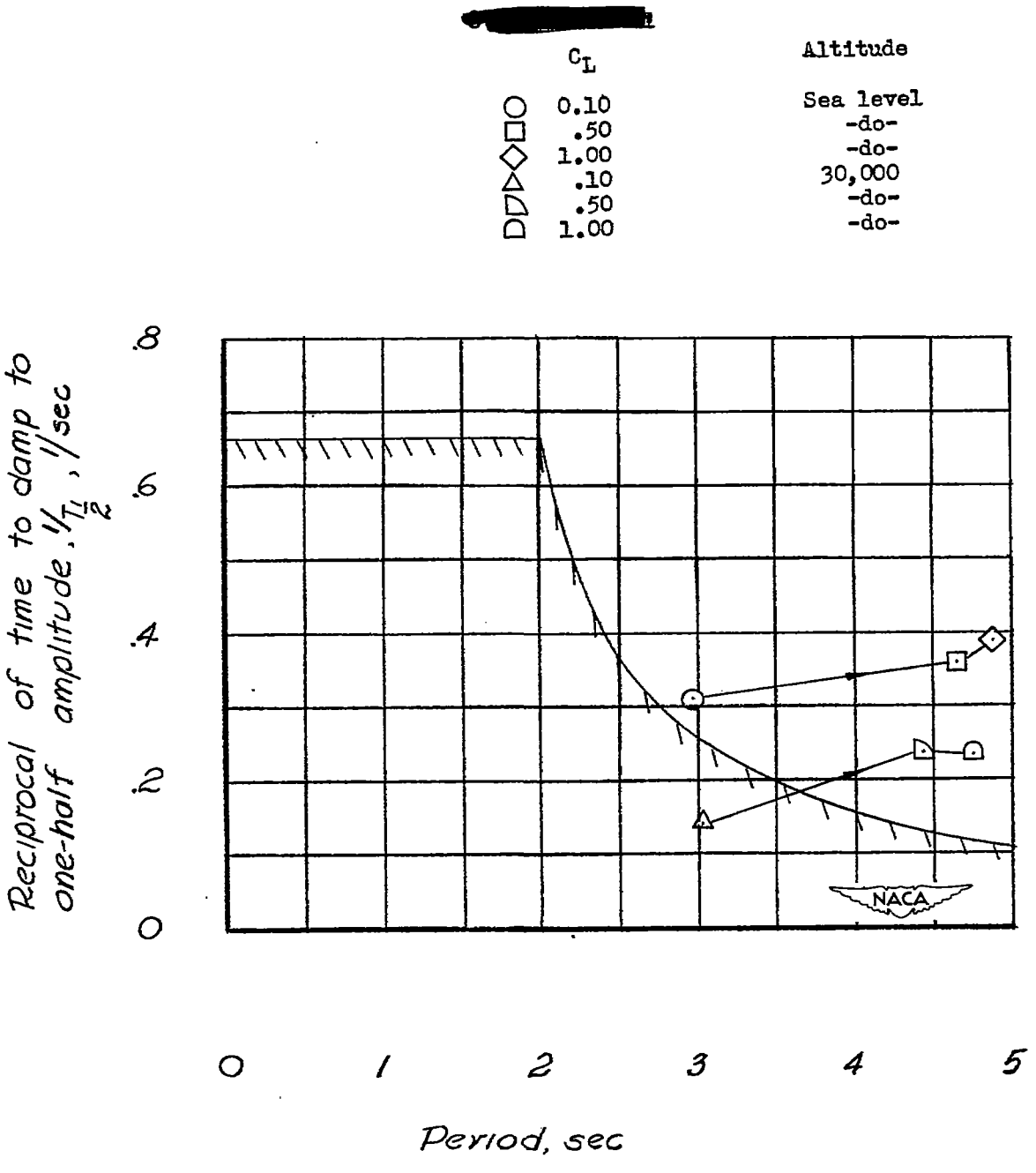

Figure 10.— Damping characteristics of the 60° triangular-wing airplane compared with the damping requirements of the U. S. Air Force.